Reconfigurable Dual-Band Bandpass Filter with Capacitive Element Insertion

Muhamad Huzaimi bin Abdul Ghafar
Faculty of Electrical Engineering
Universiti Teknologi MARA (UiTM), 40450 Shah Alam, Malaysia
huzaimi.malaysia@gmail.com

***Abstract*— These paper proposed of designing a microstrip reconfigurable dual-band bandpass filter based on an existing dual-band bandpass filter topology using High Frequency Structural Simulator (HFSS). This basic filter topology involve couple-line with transmission line forming a dual-path that produce a dual-band frequency response. Overall, the basic dual-band bandpass filter operated at center frequency 1.35 GHz and 2.71 GHz. A pair of additional lumped capacitor converted into distributed element is added at suitable location on the basic design in order to shift the frequency response. The center frequency of this filter design was shifted from 2 GHz to 1.73 GHz by varied capacitance value in order to reconfigure the frequency response.**

***Index Terms*— Dual-band, bandpass filter, tunable filter, microwave filter, center frequency, HFSS, distributed elements, lumped capacitance.**

I. Introduction

VARIOUS methods were used in designing dual-band bandpass filter such as two narrowband bandpass filter [1] combined together. The designs having different centre frequencies produce a dual-band response. A stepped-impedance resonators was then applied to obtain its higher-order resonances to form the first and second passbands [2] [3]. The semiconductor varactor method is one of the popular method used in designing a tunable dual-band band pass filter (BPF) due to its compact size, low cost and easy to be integrated with other system [4]–[6].

A tunable of dual-band band pass filter are commonly used for the multiband wireless communication and radar systems due to reduce system size and complexity [7] as well as high linearity in term of Radio Frequency Micro Electro Mechanical System (RF MEMS) technology [8]–[10]. Basically, there are three major methods used in RF MEMS which are switches and utilize semiconductor varactor. However, switches method is not usually implemented because it is very expensive and the fabrication processes are complicated [11][12].

In [13]–[16], tunable dual-band bandpass filter was designed using ferroelectric devices, piezoelectric transducer, and p-i-n diodes that can be used as well in designing a reconfigurable and tunable dual-band BPF. However, these techniques must be injected with voltage as an active element to the passband filter. Another design method of tunable filter also using by stub techniques which is just consist of redesigning the topology size.

There are three methods to design a RF MEMS devices which is active element that inject the ultra-low voltage, stub, and varactor loaded adding with semiconductor component. In [17], researcher using injection of an ultra-low voltage in designing tunable dual-band pass filter based on a pseudo-floating gate. The pseudo-floating gate is a kind of floating gate and it is biased weakly using high resistive resistors. These resistors can be made of active or passive components. However, there are some critical issues to minimize the size in this advanced technologies because it have leakages in thin oxides. The circuit enjoys low component spread and is very compact but an issue regarding the filter performance is limited by the varactor and the microstrip resonator Q [18].

In [19] and [20], researchers proposed a high-selectivity tunable dual-band bandpass filter using stub-loaded stepped-impedance resonators and constructed by using inductive coupled lumped resonator for both first passband and second passband. In the analysis, for the high-selectivity tunable dual-band bandpass filter, the researcher stated the design of T-shape open stub is able to reduce the types of control voltages in a narrow band tunable filter design, however the design method must be considerable to the size of stub which has an effect on the center frequencies of filter.

In [21], researcher Li Gao, Xiu Yin Zhang and Bin Jie Hu proposed design of tunable dual-band bandpass filter by using varactor-loaded resonator that consist both active and passive elements such as capacitor and resistor. On the result, response of tunable passband was shifted from 735 MHz to 1135 MHz, which exhibits a wide frequency range of 42.7% and the upper passband locates at 3.5 GHz with insertion loss of 1.1 dB.

In [22] , a group of researcher proposed a reconfigurable of single band filter with controllable response by adding lumped capacitors and varactors diodes. In lumped capacitor technique, researchers are used range of capacitance less than 3pF to obtain frequency response shift form the basic topology of single band filter. The center frequency of filter design shifted from 2 GHz to 984.4 Mhz.

Furthermore, in [23], researcher are used capacitance insertion and distributed element technique in order to shift frequency response on an ideal topology of dual-band bandpass filter. In this project paper, researcher was us a lumped capacitor converted to distributed elements in order to obtain the frequency response shift using Electromagnetic (EM) simulator. The capacitance value that used to shift center frequency response from 2 GHz to 1.81 GHz are around 1.1pF to 1.7pF.

This paper present, a designed microstrip line of tunable dual-band bandpass filter by adding the capacitive element that was converted to distributed elements. The center frequency shifted to the left when a higher value of a pair capacitor placed on different locations.

II. METHODOLOGY

The process flow and project plan are show in the flow chart in Figure 1.

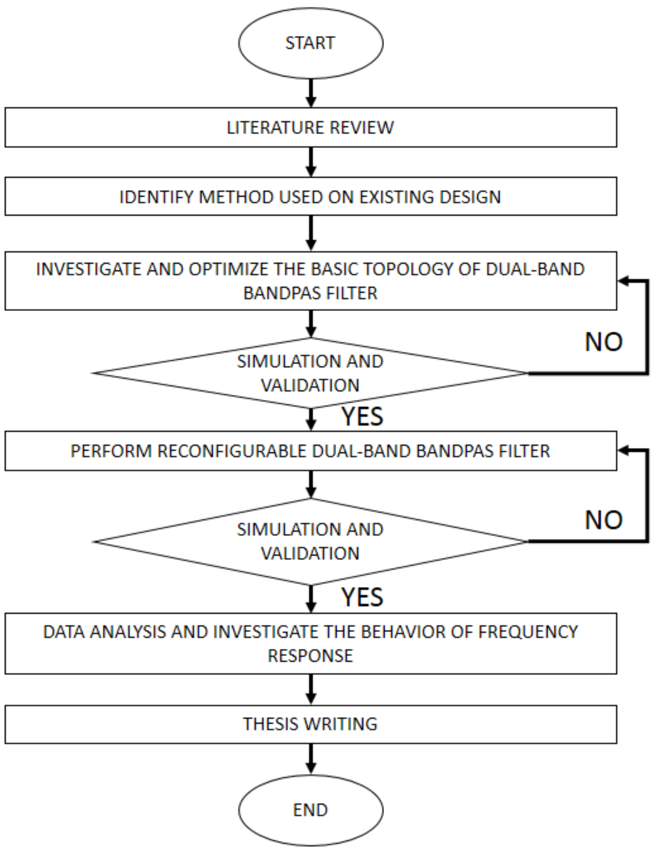

Figure 1: Flow chart for investigation the behavior of reconfigurable dual-band bandpass filter

This project focuses on identifying and characterizing the behavior of dual-band bandpass filter to obtain a suitable frequency response having reconfigurable elements. In this project the response of basic dual-band bandpass filter topology is obtained by optimizing the length and width of the transmission and couple line. The optimization process also involved the suitable location to match the center frequency from the existing design. After the basic topology response of dual-band bandpass filter is obtained, four major recommendation location of capacitor that converted to the distributed elements are investigated and the frequency responses was validated and analyzed. The center frequency shifted to the lower frequency when the bigger size of distributed elements was placed on different locations that have been stated. The length of certain capacitor used was changed to analyze the effects of response due to the different electrical length.

III. DUAL-BAND BANDPASS FILTER

The basic topology of dual-band bandpass filter as shown in Figure 2 involved three parameters which is the quarter-wavelength coupled line that connected directly with quarter-wavelength transmission line and connected parallel with another similar connection. The frequency dual-band bandpass filter was obtained by varying the value of line impedance, Z_r as well as the even and odd-mode impedance of the couple-lines, Z_{oe} and Z_{oo}. The basic response of this filter topology as shown in Figure 3 contains two band with separately by a center frequency f_o. The first passband center frequency indicated as f_1 while the second passband frequency as f_2. There are three transmission zero containing in this response for better selectivity of frequency.

Simulation for the basic topology was performed using HFSS in 3 Dimension (3D) form. The design was implemented on ROGER TMM10 substrate with relative dielectric constant, ε_r = 9.2, substrates thickness h = 1.27 mm and tangent loss, tan δ = 0.0022. The center frequency, f_o was achieved at 2 GHz with the first frequency f_1 = 0.97 GHz and second frequency, f_2 = 3.12 GHz for the two passbands respectively. Figure 3 shows the frequency response, transmission zero and rejection band of basic filter topology. Transmission zero for this design are indicated at -52.13 dB for center frequency, -42.13 dB (first passband), and -27.81 dB (second passband). Meanwhile, the band rejection for this dual-band bandpass filter are less than 0.99 GHz for lower rejection band more than 3.13 GHz for the upper rejection band.

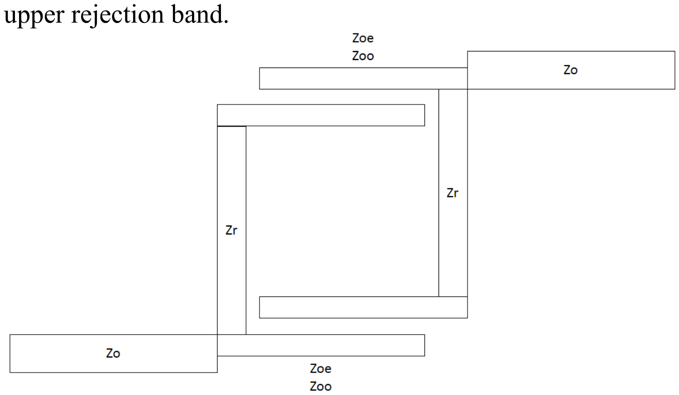

Figure 2: Layout of the basic dual-band bandpass filter topology

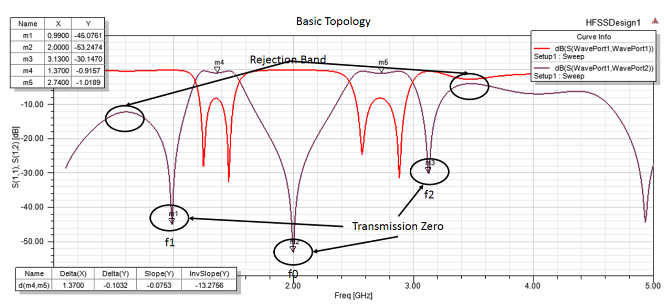

Figure 3: Frequency response of the basic topology dual-band bandpass filter

The three parameters of basic topology was determined by seven different sizes of width and length including the gap. Both of thres parameters were vared in term of witdh and length to obtain the center frequency of 2 GHz. Figure 4 shows the exact location of each parameter with their width and length. L_{io} and W_{io} are indicated as the length and width of the input and output of 50 Ω feed-line, Z_o. L_r and W_r are indicated as the length and width for line impedance, Z_r. Meanwhile, L_c, W_c and G are represent the length, width and gap for coupled line, Z_{oe} and Z_{oo} respectively. Table 1 shows size of all width and length.

TABLE 1
WIDTH AND LENGTH OF BASIC TOPOLOGY PARAMETERS

Parameters	Size (mm)
L_{io}	14.9933
W_{io}	1.3152
L_r	15.2088
W_r	0.92253
L_c	15.11959
W_c	1.0795
G	0.762

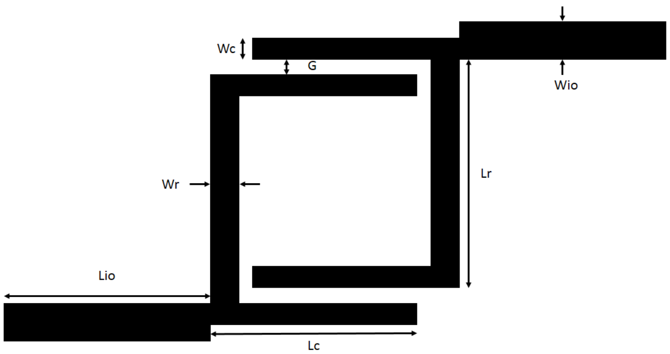

Figure 4: Layout of microstrip line dual-band bandpass filter.

Figure 5(a), 5(b), 5(c), 5(d) and 5(e) shows the behavior of frequency response when one of the parameter in Table 1 increase while others were remain constant. As shown in Figure 5(a), transmission zero of first and second passband shift to the left while center frequency remain 2 GHz when L_r increase. Meanwhile, Figure 5(b) shows the transmission zero of both first and second passband shifted to right when varied W_r. Figure 5(c) and Figure 5(d) shows all transmission zero for center frequency first, second passband shifted to the left when increase L_c and W_c. Meanwhile, by increasing the gap, the frequency response move downward to the lower magnitude. By varying the value of gap, it also changes the filter response amplitude. Therefore, by changing value of length, the filter frequency was shifted while controlling the value of width, it can be seen that the frequency shift with changes in amplitude.

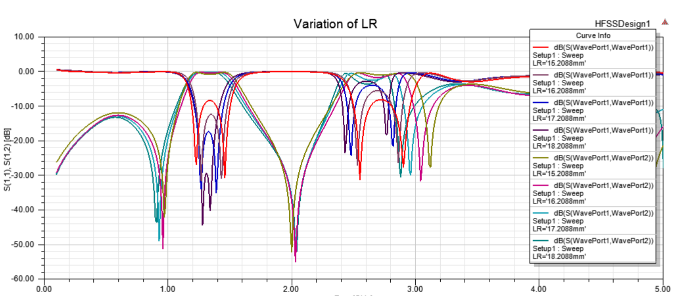

Figure 5(a): Response with variations of L_r

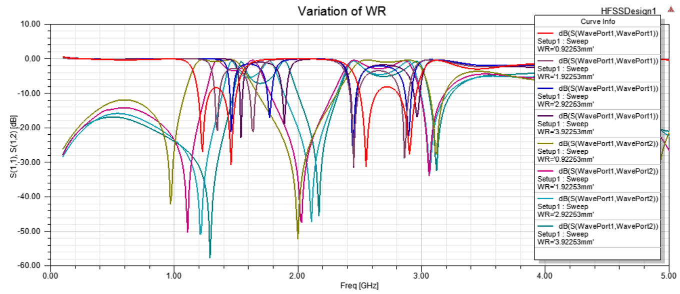

Figure 5(b): Response with variations of W_r

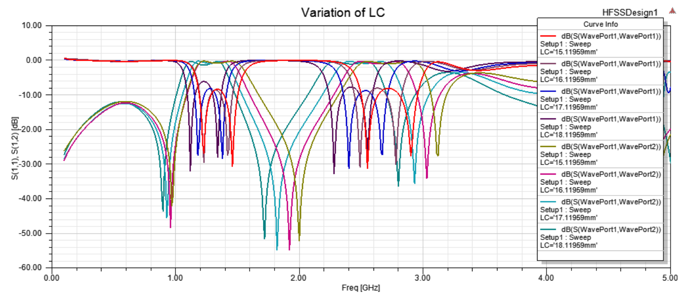

Figure 5(c): Response with variations of L_c

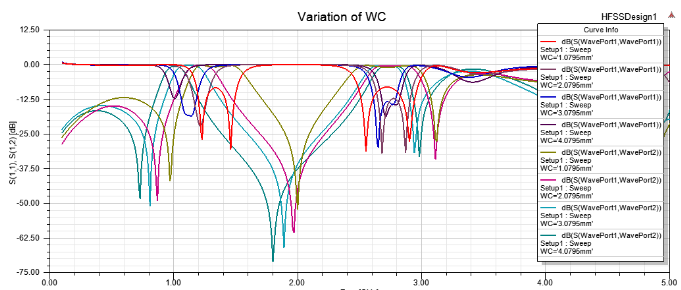

Figure 5(d): Response with variations of W_c

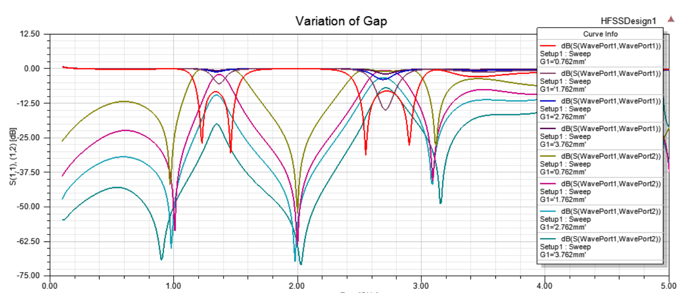

Figure 5(e): Response with variations of gap

IV. RECONFIGURABLE DUAL-BAND BANDPASS FILTER

A. *Capacitive elements*

This proposed dual-band bandpass filter need to adopt a pair capacitive elements in order to obtain it reconfigurable effect. This capacitive elements were placed diagonally in four different location on basic topology filter as shown in Figure 6. The varying four different location is to choose the suitable location to place in the capacitive elements. Before the capacitive element added into the topology, it need to convert in distributed elements which varying in term of width and length of microstrip line. The calculation width and length of microstip line are based on the formula as shown below.

$$X_C = \frac{1}{2\pi f c} \quad (1)$$

$$\frac{W}{d} = \begin{cases} \frac{8e^A}{e^{2A}-2} & \text{For W/d <2} \\ \frac{2}{\pi}\left[B-1-\ln(2B-1)+\frac{\varepsilon_r-1}{2\varepsilon_r}\left\{\ln(B-1)+0.39-\frac{0.61}{\varepsilon_r}\right\}\right] & \text{For W/d >2} \end{cases} \quad (2)$$

$$A = \frac{Z_c}{60}\sqrt{\frac{\varepsilon_r+1}{2}}+\frac{\varepsilon_r-1}{\varepsilon_r+1}\left(0.23+\frac{0.11}{\varepsilon_r}\right) \quad (3)$$

$$B = \frac{377\pi}{2Z_o\sqrt{\varepsilon_r}} \quad (4)$$

$$\beta l = \sqrt{\varepsilon_r}k_o f \quad (5)$$

$$k_o = \frac{2\pi f}{c} \quad (6)$$

c = $3x10^8$ (speed of light)

$$l = \frac{\emptyset(\frac{\pi}{180})}{\sqrt{\varepsilon_r}k_o} \quad (7)$$

The value of capacitance Z_c was determine by using (1), before calculated it into the width and length of distributed elements using formula (2) and (7). The value of f and $\mathcal{E}_r$ is center frequency and dielectric constant of design filter. Phase shift is indicated with $\emptyset = 90^{\circ}$. However the length of the distributed elements were varied to investigate the best frequency response, band rejection and number of modes of signal. However, length for each location were varied not less than 2 mm to perform the suitable result of dual-band bandpass filter.

Figure 7(a) and 7(b) shows the frequency response with added capacitive elements C=1.1pF at location in Figure 6. The width and length of each pair distributed elements which is placed in four different location were assigned as 552.62 µm and 1.9352 mm respectively.

Figure 7(a) shows center frequency of dual-band bandpass filter shift to 1.94 GHz while first and second passband also shifted from 0.99 GHz to 0.96 GHz and 3.13 GHz to 3.08 GHz respectively. The frequency response of distributed elements as shown in Figure 7(b) give the maximum shift for center frequency from 2 GHz to 1.86 GHz and the first passband remain 0.99 GHz. However, it second passband shifted from 3.13 GHz to 3.12 GHz.

The center frequency for distributed elements at location 2 as shown in Table 2 remain at 2 GHz while first and second passband shifted from 0.99 GHz to 0.96 GHz and 3.13 GHz to 3.08 GHz respectively. Meanwhile, the distributed elements at location 4 as tabulated in Table 2 remain the center frequency at 2 GHz while first passband shifted from 0.99 GHz to 0.96 GHz and second passband from 3.13 GHz to 3.06 GHz.

Therefore, location 3 has been chosen for possible configuration of distributed elements on because it give the maximum shift for basic dual-band bandpass filter. All frequency shifted causing of distributed elements were tabulated in Table 2.

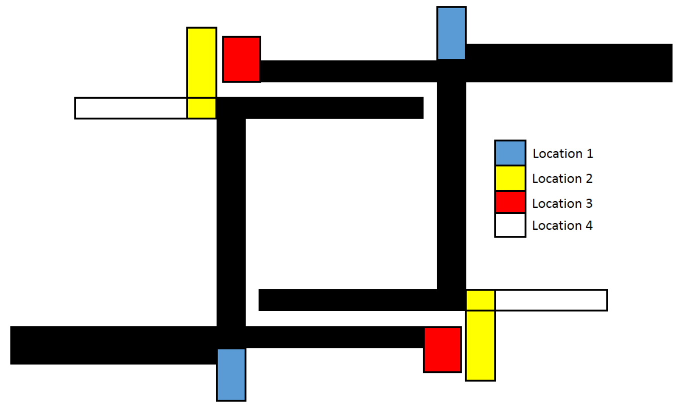

Figure 6: Four recommendation location of a pair capacitive elements

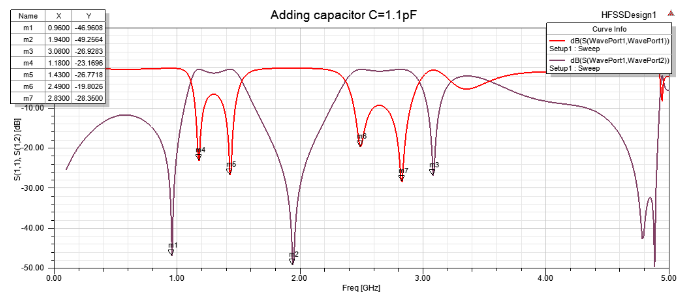

Figure 7(a): Frequency response with distributed elements at location 1

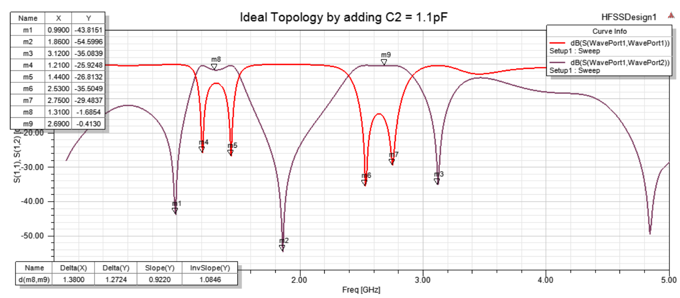

Figure 7(b): Frequency response with distributed elements at location 3

TABLE 2
FREQUENCY WITH DIFFERENT LOCATION OF DISTRIBUTED ELEMENTS

Location	f_1 (GHz)	f_0 (GHz)	f_2 (GHz)
Basic	0.99	2.00	3.13
1	0.96	1.94	3.08
2	0.97	2.00	3.08
3	0.99	1.86	3.12
4	0.96	2.01	3.06

B. Optimization of Capacitive Elements

In order to obtain wider frequency shift, capacitive element was optimized based on the width and length. The optimization on this elements is depend to the capacitance value. Figure 8 shows the frequency response after added capacitive element at location that has been chosen before with variation value of capacitance. The width and length indicated for C=1pF is 419.86 µm and 1.9512 mm, C=1.1pF (552.62 µm and 1.9352 mm), C=1.2pF (695.73 µm and 1.9206 mm), C=1.5pF (1.16 mm and 1.88369 mm), C=1.6pF (1.33 mm and 1.87331 mm), C=1.7pF (1.5 mm and 1.86373 mm) and C=2pF (2.01 mm and 1.8388 mm).

Result in Table 3 shows frequency response after adopting capacitive elements C=1pF to C=2pF. In C=1pF, it recorded center frequency shifted 7% from the ideal response. Meanwhile after added C=2pF, the center frequency shifted from 2 GHz to 1.73 GHz or 13.5% shifting from the original value. High value of capacitance shifted more the center frequency to the left. Therefore, capacitance increase, percentage of shifting increase. This result shows narrow down the width band of first passband while increase width of second passband.

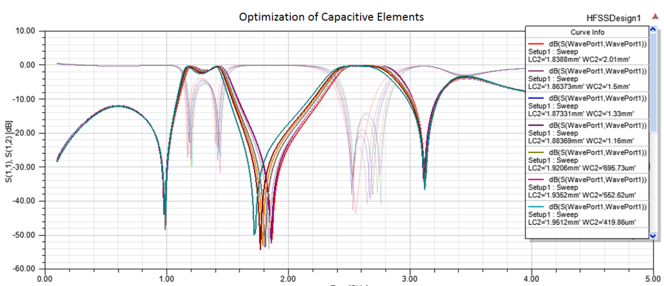

Figure 8: Frequency response with variation of capacitance

TABLE 3
FREQUENCY WITH DIFFERENT CAPACITIVE ELEMENTS

Capacitance (pF)	f_1 (GHz)	f_0 (GHz)	f_2 (GHz)	Percentage (%)
Basic	0.99	2.00	3.13	0.00
1.0	0.99	1.86	3.12	7.00
1.1	0.99	1.86	3.12	7.00
1.2	0.99	1.84	3.12	8.00
1.5	0.99	1.81	3.12	9.50
1.6	0.99	1.79	3.12	10.50
1.7	0.99	1.77	3.12	11.50
2.0	0.99	1.73	3.12	13.50

V. RESULT AND DISCUSSION

All simulation was executed by 3 Dimension dual-band bandpass filter using High Frequency Structural Simulator. The frequency response result of basic topology and reconfigurable dual-band bandpass filter is shown in Figure 9 and Figure 10 respectively. The design was implemented on ROGER TMM10 type of substrate which have relative dielectric constant, ε_r = 9.2, substrates thickness h = 1.27 mm and tangent loss, tan δ = 0.0022. By using capacitor value C=1.6pF which converted to distributed element at the suitable location, the center frequency shifted to lower frequency response from 2 GHz to 1.79 GHz. The frequency was shifted around 210 MHz. However, the first passband remain unchanged at 0.99 GHz while the second passband shifted around 10 MHz from 3.13 GHz to 3.12 GHz. The resulting of the frequency response shift was narrowed down the width band of first passband.

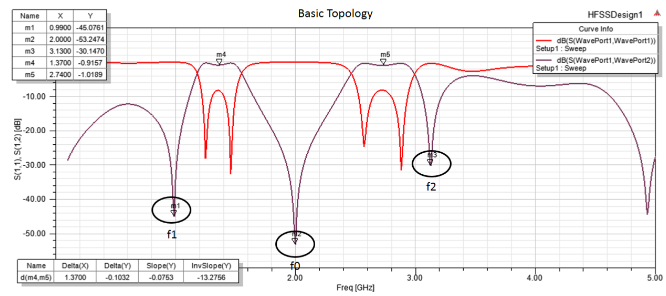

Figure 9: Frequency response of basic topology

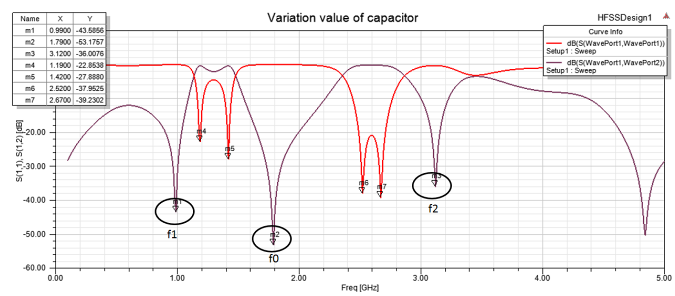

Figure 10: Frequency response by adding distributed element

VI. CONCLUSION

As a conclusion, a microstrip line of reconfigurable dual-band bandpass filter has been designed with adding capacitive elements which are converted into distributed elements. The filter design was investigated with different locations of distributed elements towards the greater center frequency shift. The investigation was performed in four different location which were indicated to obtain the suitable location of capacitive elements. Then, the design optimized it by using seven variation of capacitance value with same location to verifying how much shifted if added bigger value of capacitance.

VII. ACKNOWLEDGMENT

I would like to express my sincere gratitude to my main supervisor, Dr Zuhani binti Ismail Khan for continuous support to finish my master project. She always guides me with in term of the fundamental of tunable dual-band bandpass filter. Her patience, motivation and immense knowledge help me in many ways to finish the project.

VIII. References

[1] H. Miyake, S. Kitazawa, T. Ishizaki, T. Yamada, and Y. Nagatomi, "A miniaturized monolithic dual band filter using ceramic lamination technique for dual mode portable telephones," *IEEE MTT-S Int. Microw. Symp. Dig.*, vol. 2, pp. 789–792, 1997.

[2] W. S. Chang and C. Y. Chang, "Analytical design of microstrip short-circuit terminated stepped-impedance resonator dual-band filters," *IEEE Trans. Microw. Theory Tech.*, vol. 59, no. 7, pp. 1730–1739, 2011.

[3] S. Sun and L. Zhu, "Compact dual-band microstrip bandpass filter without external feeds," *IEEE Microw. Wirel. Components Lett.*, vol. 15, no. 10, pp. 644–646, 2005.

[4] X. Y. Zhang and Q. Xue, "High-Selectivity Tunable Bandpass Filters," vol. 58, no. 4, pp. 964–969, 2010.

[5] J. Lee and K. Sarabandi, "An analytic design method for microstrip tunable filters," *IEEE Trans. Microw. Theory Tech.*, vol. 56, no. 7, pp. 1699–1706, 2008.

[6] M. A. El-Tanani and G. M. Rebeiz, "A two-pole two-zero tunable filter with improved linearity," *IEEE Trans. Microw. Theory Tech.*, vol. 57, no. 4, pp. 830–839, 2009.

[7] G. Chaudhary, Y. Jeong, and J. Lim, "Harmonic suppressed dual-band bandpass filters with tunable passbands," *IEEE Trans. Microw. Theory Tech.*, vol. 60, no. 7, pp. 2115–2123, 2012.

[8] K. Entesari and G. M. Rebeiz, "A differential 4-bit 6.5-10-GHz RF MEMS tunable filter," *IEEE Trans. Microw. Theory Tech.*, vol. 53, no. 3 II, pp. 1103–1110, 2005.

[9] A. Pothier *et al.*, "Low-loss 2-bit tunable bandpass filters using MEMS DC contact switches," *IEEE Trans. Microw. Theory Tech.*, vol. 53, no. 1, pp. 354–360, 2005.

[10] K. Entesari and G. M. Rebeiz, "A 12-18-GHz three-pole RF MEMS tunable filter," *IEEE Trans. Microw. Theory Tech.*, vol. 53, no. 8, pp. 2566–2571, 2005.

[11] V. Sekar, M. Armendariz, and K. Entesari, "A 1.2–1.6-GHz Substrate-Integrated-Waveguide RF MEMS Tunable Filter," *IEEE Trans. Microw. Theory Tech.*, vol. 59, no. 4, pp. 866–876, 2011.

[12] I. Reines, S. J. Park, and G. M. Rebeiz, "Compact low-loss tunable X-band bandstop filter with miniature RF-MEMS switches," *IEEE Trans. Microw. Theory Tech.*, vol. 58, no. 7 PART 1, pp. 1887–1895, 2010.

[13] J. Nath *et al.*, "An electronically tunable microstrip bandpass filter using thin-film Barium-Strontium-Titanate (BST) varactors," *IEEE Trans. Microw. Theory Tech.*, vol. 53, no. 9, pp. 2707–2712, 2005.

[14] I. Vendik, O. Vendik, V. Pleskachev, A. Svishchev, and R. Wordenweber, "Design of tunable ferroelectric filters with a constant fractional band width," pp. 1461–1464, 2001.

[15] L. Hsieh and K. Chang, "Tunable microstrip bandpass filters with two transmission zeros," *Microw. Theory Tech. IEEE Trans.*, vol. 51, no. 2, pp. 520–525, 2003.

[16] B. Liu, F. Wei, and X. Shi, "Reconfigurable bandpass filter based on net-type stepped-impedance resonator," *Electron. Lett.*, vol. 46, no. 22, p. 1506, 2010.

[17] M. Azadmehr, B. K. Khajeh, and Y. Berg, "An ultra-low voltage tunable dual-Band Pass Filter," *2014 IEEE 11th Int. Multi-Conference Syst. Signals Devices, SSD 2014*, no. I, pp. 4–8, 2014.

[18] T. Yang and G. M. Rebeiz, "Three-Pole 1.3-2.4-GHz Diplexer and 1.1-2.45-GHz dual-band filter with common resonator topology and flexible tuning capabilities," *IEEE Trans. Microw. Theory Tech.*, vol. 61, no. 10, pp. 3613–3624, 2013.

[19] B. You, L. Chen, Y. Liang, and X. Wen, "A high-selectivity tunable dual-band bandpass filter using stub-loaded stepped-impedance resonators," *IEEE Microw. Wirel. Components Lett.*, vol. 24, no. 11, pp. 736–738, 2014.

[20] Y. H. Cheng, H. S. Peng, and Y. C. Chiang, "Design of tunable dual-band filter with multiple types of resonators," *Eur. Microw. Week 2015 "Freedom Through Microwaves", EuMW 2015 - Conf. Proceedings; 2015 45th Eur. Microw. Conf. Proceedings, EuMC*, pp. 415–418, 2015.

[21] L. Gao, X. Y. Zhang, and B. J. Hu, "Tunable dual-band bandpass filter using varactor-loaded short-ended resonators," *2013 IEEE Int. Wirel. Symp. IWS 2013*, no. April 2013, pp. 1–4, 2013.

[22] N. Ab Wahab, M. K. Mohd Salleh, Z. Ismail Khan, and N. E. Abd Rashid, "Reconfigurable ring filter with controllable frequency response," *Sci. World J.*, vol. 2014, 2014.

[23] Wan Nurul Shuhada binti Wan Deraman, "Tunable Dual-Band Bandpass Filter," Universiti Teknologi MARA, 2015.